Scientia Iranica B (2016) 23(1), 238–248

SCIENTIA IRANICA

Sharif University of Technology
Scientia Iranica
Transactions B: Mechanical Engineering
www.scientiairanica.com

Probing into the effects of fuel injection pressure and nozzle hole diameter on spray characteristics under ultra-high injection pressures using advanced breakup model

M. Yousefifard[a], P. Ghadimi[a,*] and S.M. Mirsalim[b]

a. *Department of Marine Technology, Amirkabir University of Technology, Tehran, Iran.*
b. *Department of Mechanical Engineering, Amirkabir University of Technology, Tehran, Iran.*

Received 27 June 2014; received in revised form 9 November 2014; accepted 13 April 2015

KEYWORDS
Diesel spray;
Ultra-high injection pressure;
Nozzle hole diameter;
Penetration length;
Breakup model;
OpenFOAM.

Abstract. In this article, non-evaporating and non-reacting diesel spray is modeled under ultra-high injection pressure using an Eulerian-Lagrangian scheme. This is accomplished in order to probe into the effects of injection pressure, nozzle diameter, and ambient density on spray characteristics. An advanced hybrid breakup model that takes into consideration the transient processes during spray injection has been added to the open source code, OpenFOAM. Reynolds-Average Navier-Stokes (RANS) equations are solved using the standard $k-\varepsilon$ turbulence model and the fuel droplet is tracked by a Lagrangian scheme. Published experimental data have been used for validation of spray characteristics at 15 kg/m^3 ambient density and injection pressures of 100, 200 and 300 MPa. Also, three nozzle diameters of 0.08, 0.12 and 0.16 mm have been implemented for investigating the effect of this parameter on spray formation. Computed spray shape, jet penetration, spray volume, equivalent ratio along the injector axis and Sauter Mean Diameter (SMD) illustrate good agreement with experimental data of a single hole nozzle and symmetric spray. The effects of fuel injection pressure, nozzle hole diameter and ambient density on main spray parameters are presented. It is concluded that the numerical model presented here is quite suitable for accurately predicting diesel spray shapes under ultra-high injection pressures.

1. Introduction

Pollution and efficiency in diesel engines are greatly influenced by the quality of atomization and the fuel-air mixture. Injection and chamber pressures are two of the most important parameters affecting fuel atomization. Moreover, the fuel injection pressure of Direct Injection (DI) engines has continued to increase in recent years, and it has, therefore, become necessary to take an interest in modeling ultra-high injection pressures (above 100 MPa). The mechanism of fuel atomization is extremely complicated, and this multiphase flow consists of a large number of phenomena, such as cavitation, breakup, evaporation, and reaction. Among these phenomena, the majority of past numerical modeling has involved research into the breakup of droplets during the injection process. Specifically, increasing the injection pressure leads to some complicated breakup phenomena that should be simulated by an advanced model.

Recently, Computational Fluid Dynamics (CFD) has played a major role in engine development in automotive and marine industries. Its application as an engine development tool can be dated back to

*. *Corresponding author. Tel.: +98 21 64543117; Fax: +98 21 66412495*
E-mail address: pghadimi@aut.ac.ir (P. Ghadimi)

the early 1980's with considerable development in the second part of the 1990s [1]. The Eulerian-Lagrangian scheme is a proper choice to conduct spray simulation in diesel engines. Moreover, in most literature related to spray simulation under Eulerian-Lagrangian formulation, the atomization process can be divided into two procedures; primary and secondary breakup. On the other hand, several theoretical studies, in particular those based on surface instabilities, have been developed. Liquid spray breakup can be caused by Kelvin-Helmholtz (KH) and Rayleigh-Taylor (RT) instabilities at the interface of two fluids. KH instability is due to high shear at the interface, while the RT breakup theory is based on the stability of liquid-gas interfaces during acceleration in the normal direction to the plane. Most commonly used breakup models are based on KH and RT theories [2].

There has been much research into the numerical modeling of diesel spray that has focused on breakup and atomization phenomena. Spray penetration has been investigated numerically by Wan and Peters [3]. Som and Aggarwal [4] performed 3-D simulations with detailed chemistry using a new advanced breakup model. Hosseinpour and Binesh [5] also used a CFD code to investigate the effect of a breakup model on spray and mixture formation in a heavy-duty diesel engine. Som et al. [6] reported a computational investigation of internal nozzle flow and cavitation characteristics in a diesel injector. Ishii et al. [7] presented a method that combines two types of simulation, based on the particle method, for simulation of liquid-film breakup near the injector outlet, and a discrete droplet model for the secondary-drop breakup. Desantes et al. [8] developed a model which is able to predict spray tip penetration and spray axis velocity. Recently, Turner et al. [9] proposed a breakup model for analyzing the evolution of transient fuel. Also, Yadollahi and Boroomand [10] used AVL FIRE software to perform an investigation into direct injection of natural gas into the cylinder of spark ignition internal combustion engines. Mohammadebrahima et al. [11] simulated in-cylinder flow using ANSYS FLUENT software. Ghasemi et al. [12] presented a numerical study on the spray-induced air motion in single and twin ultra-high injection diesel sprays using ANSYS FLUENT software.

Ultra-high pressure injection has been the aim of some recent studies. Kato et al. [13] and Yokota et al. [14] experimentally examined the effects of injection pressure ranging from 55 to 250 MPa. An experimental research study was carried out by Benajes et al. [15] to analyze the influence of different orifice geometries on the injection rate of a common-rail fuel injection system. On the other hand, Kastengren et al. [16] experimentally studied the effects of nozzle geometry and injection duration on diesel spray.

Ultra-high injection pressure has also been studied by Lee et al. [17], experimentally and numerically, up to 355 MPa. Tao and Bergstrand [18] investigated the effect of very high injection pressures on engine ignition and combustion using three-dimensional numerical simulations. Wang et al. [19] presented a detailed experimental inspection of diesel and biodiesel spray characteristics for high injection pressure up to 300 MPa. The effect of ambient pressure on the penetration of a diesel spray was investigated experimentally and theoretically by Roisman et al. [20]. Also, Zhu et al. [21] experimentally investigated the effects of fuel injection pressure, ambient gas density and nozzle hole diameter on the surrounding gas flow of a single diesel spray under ultra-high injection pressures.

Shervani-Tabar et al. [22] have also carried out a numerical simulation to study the effect of injection pressure on spray penetration length.

Recently, open source codes have been utilized as efficient methods for modeling diesel spray by researchers like Gjesing et al. [23], Kassem et al. [24], Vuorinen et al. [25], Nowruzi et al. [26] and Yousefifard et al. [27,28], among others. KIVA and OpenFOAM software are becoming popular as open source codes in this field of interest. Accordingly, in the current study, non-evaporating spray characteristics of an ultra-high injection pressure diesel spray are studied under injection pressures up to 300M Pa by the OpenFOAM freeware code. The SprayFoam solver has been applied to consider the compressibility effect of air, and a modified breakup model has been added to the default solver to achieve more accurate results at ultra-high injection pressures. A Lagrangian particle tracking approach has been employed using a new and advanced KH-RT breakup model to accurately simulate direct injection of fuel at very high pressures. Spray tip penetration, spray angle and spray volume have been computed and compared against available experimental results.

Governing equations in two-phase flow are presented first, and the current spray breakup model is discussed in more depth. Subsequently, details of experimental data that are used to validate the current model are presented. Later, computed results are analyzed and compared against experimental data. Finally, the advantages of the current scheme in simulating ultra-high injection pressure have been presented in the conclusions.

2. Governing equations

Mathematical models of fluid flow and heat transfer are generally developed according to conservation laws of physics, such as the conservation of mass, Newton's second law, and the first law of thermodynamics [29]. Compressible flows can be expressed by Navier-Stokes (NS) equations describing the conservation of mass,

momentum and energy. Navier-Stokes equations for conservative variables of a continuous field are as follows [30]:

a) Equation of mass conservation:

$$\frac{\partial \rho}{\partial t} + \frac{\partial}{\partial x_j}(\rho u_j) = 0, \tag{1}$$

where ρ denotes the fluid density, x_j is the jth component of the Cartesian coordinates, and u_j represents the jth component of the fluid velocity.

b) Equation of momentum conservation:

$$\frac{\partial}{\partial t}(\rho u_i) + \frac{\partial}{\partial x_j}(\rho u_j u_i) = -\frac{\partial P}{\partial x_i} + \frac{\partial}{\partial x_j}\left(\tau_{ij} + \tau_{ij}^R\right), \tag{2}$$

where $P \equiv p + \rho g z$ is the modified pressure variable, p is the pressure, g represents body force, and $\tau = \tau_{ij}$ denotes the stress tensor [31].

$$\tau_{ij} = -p\delta_{ij} + 2\mu S_{ij},$$

$$S_{ij} = \frac{1}{2}\left(\frac{\partial u_i}{\partial x_j} + \frac{\partial u_j}{\partial x_i}\right). \tag{3}$$

S_{ij} is the rate-of-strain tensor

$$\tau_{ij}^R = -\rho\overline{u_i' u_j'}. \tag{4}$$

c) Equation of energy conservation:

$$\frac{\partial \rho E}{\partial t} + \frac{\partial(\rho E u_i)}{\partial x_j} = -\frac{\partial q_j}{\partial x_j} + \rho g_i u_i + \frac{\partial}{\partial x_j}(p u_j) + \frac{\partial}{\partial x_i}(\tau_{ij} u_j). \tag{5}$$

Here, E denotes the total energy per unit volume, q_j is the jth component of the heat flux vector, q. Favre time averaging is applied to the flow variables. The PISO algorithm [32] is used for the pressure-velocity coupling, and the standard $k-\varepsilon$ turbulence model [33] is applied in RANS modeling.

To capture the turbulence characteristics of the flow, there are three important approaches for simulation of turbulent flows: Reynolds Average Navier-Stokes (RANS), Large-Eddy Simulations (LES) and Direct Numerical Simulation (DNS). Among these, RANS is still favorite in flow simulation due to its economy, robustness and reasonable accuracy in a wide range of turbulent flows. The standard $k-\varepsilon$, which is a classical turbulence model within RANS and is based on transport equations for turbulence kinetic energy (k) and its dissipation rate (ε), has been adopted for the current study.

The Lagrangian Particle Tracking (LPT) approach is usually employed for spray simulation. In the current simulation, the motion of particles is governed by Newton's equation of motion. It is assumed that the force acting on a droplet due to a drag will be given as:

$$\frac{1}{6}\rho_p \pi d^3 \frac{du_p}{dt} = \frac{1}{2}(u_g - u_p)\,|u_g - u_p|\,\rho_g C_D \frac{\pi d^2}{4}, \tag{6}$$

where u_p is the particle velocity, u_g is the gas velocity that is interpolated to the particle position from the adjacent cells, and C_D is the droplet drag coefficient defined by:

$$C_D = \begin{cases} \frac{24}{\mathrm{Re}_p}\left(1 + \frac{1}{6}\mathrm{Re}_p^{2/3}\right) & \mathrm{Re}_p < 1000 \\ 0.424 & \mathrm{Re}_p \geq 1000 \end{cases} \tag{7}$$

The droplet Reynolds number is given by $\mathrm{Re}_p = \frac{|u_g - u_p| d}{v_g}$.

Several sub-models, such as droplet breakup and collision, should be used in spray modeling. As noted before, the breakup process is described by the aerodynamic stripping of small droplets from the larger droplets (Kelvin-Helmholtz instability) or the disintegration of large droplets into smaller ones due to the effect of normal stresses (Rayleigh-Taylor instability). The Kelvin-Helmholtz wave is driven by aerodynamic forces among gas liquid phases, whereas the Rayleigh-Taylor wave is the result of acceleration of shed droplets ejected into free-stream conditions. The current hybrid model combines the effects of Kelvin-Helmholtz (KH) waves with Rayleigh-Taylor (RT) instabilities [34]. In the KHRT model, aerodynamic force on the drop flattens it into the shape of a liquid sheet, and the decelerating sheet breaks into large-scale fragments by means of RT instability. KH waves with a much shorter wavelength originate at the edges of fragments and break up into micrometer-size drops.

The growth of KH instabilities on the liquid surface at the interface of two phases that have different densities, causes "child" droplets to be stripped from the liquid core of the jet, which is approximated by "parent" droplets. Radius, r_d, of the injected droplet is assumed to continuously decrease in size during the breakup process, as described by the following equation:

$$\frac{dr_d}{dt} = -\frac{r_d - r_s}{\tau_{bu}}, \tag{8}$$

where τ_{bu} is the characteristic breakup time of the droplet, and r_s is the radius of stable droplets, given by:

$$r_s = \begin{cases} \beta_0 \Lambda & B_0\Lambda \leq r_d \\ \min\begin{pmatrix} (3\pi r_d^2 U_m/2\Omega)^{0.33} \\ (3r_d^2\Lambda/4)^{0.33} \end{pmatrix} & B_0\Lambda > r_d \end{cases} \tag{9}$$

where $B_0 = 0.61$ is the model constant, and Λ and Ω are wave-length and growth rate of the fastest growing wave on the surface of the liquid jet, respectively, given by:

$$\Omega_{KH} = \sqrt{\frac{\sigma}{\rho_l r_0^3}}.\frac{0.34 + 0.38\mathrm{We}_g^{1.5}}{(1+\mathrm{Oh})(1+1.4\mathrm{Ta}^{0.6})}, \tag{10}$$

$$\Lambda_{KH} = 9.02 r_0.\frac{(1+0.45\sqrt{\mathrm{Oh}})(1+1.4\mathrm{Ta}^{0.7})}{(1+0.865\mathrm{We}_g^{1.67})^{0.6}}, \tag{11}$$

where:

$$\mathrm{Oh} = \frac{\sqrt{\mathrm{We}_l}}{\mathrm{Re}_l}, \quad \mathrm{Ta} = \mathrm{Oh}\sqrt{\mathrm{We}_g},$$

$$\mathrm{We}_g = \frac{\rho_g r_0 u_{rel}^2}{\sigma}, \quad \mathrm{We}_l = \frac{\rho_l r_0 u_{rel}^2}{\sigma},$$

$$\mathrm{Re}_l = \frac{\rho_l r_0 u_{rel}}{\mu_l}, \tag{12}$$

r_0 is the droplet radius before breakup, $u_{rel} = |u_d - u|$ is the relative velocity between the droplet and surrounding gas, Oh is the Ohnesorge number, Ta is the Taylor number, We_g and We_l are the Weber numbers for liquid and gas, respectively, and Re_l is the Reynolds number for liquid.

Also, the breakup time is given by:

$$\tau_{bu} = 3.7626\frac{B_1 R}{\Lambda\Omega}, \tag{13}$$

where B_1 is an adjustable model constant which varies approximately between $\sqrt{3}$ and 60, depending upon the injector type. A higher value of B_1 leads to a reduced breakup and increased penetration, while a smaller value, on the other hand, results in an increased spray disintegration, a faster fuel-air mixing, and reduced penetration. The default value of B_1 in the software is $B_1 = 40$, and some higher values up to 60 have been suggested. This model was modified to incorporate transient effects by Sazhin et al. [35]. The modified WAVE breakup model introduced new breakup time. The model constant in Eq. (13) has been modified to:

$$B_1^{\mathrm{mod}} = B_1\left(1 + C_1(a^+)^{C_2}\right), \tag{14}$$

where:

$$a^+ = 2\sqrt{\mathrm{Re}_2}\frac{r_d}{U_{inj}^2}\frac{dU_{inj}}{dt}, \tag{15}$$

is the acceleration parameter, C_1 and C_2 are adjustable model constants, and Re_2 is the gas Reynolds number.

RT instabilities appear when acceleration is normal to the interface of two fluids with different densities. Similar to KH instabilities, the wavelength and growth rate of the fastest growing wave can be obtained from linear stability analysis. The growth rate of the fastest growing wave and the corresponding wave length of the Rayleigh-Taylor model are given by Bellman and Pennington [36], as in:

$$\Omega_{RT} = \sqrt{\frac{2}{3\sqrt{3\sigma}}\frac{[a(\rho_l - \rho_g)]^{3/2}}{\rho_l - \rho_g}}, \tag{16}$$

$$\Lambda_{RT} = C_3 2\pi\sqrt{\frac{3\sigma}{a(\rho_l - \rho_g)}}. \tag{17}$$

For the current numerical model, both instability models are utilized simultaneously and breakups are determined by the fastest growth rate of waves. In this equation, a is the droplet acceleration given as:

$$a = \frac{3}{8}C_D\frac{\rho_g u_{rel}^2}{\rho_l r}. \tag{18}$$

Figure 1 illustrates the schematic diagram of the breakup mechanism in the KH and RT models.

The KHRT model is the most popular of all hybrid breakup models. It has been successfully validated against experimental data and used by many authors in order to predict the disintegration process of high-pressure diesel sprays [1].

In the current study, the modified WAVE breakup model that was introduced by Sazhin et al. [35] has been implemented, and a new advanced KHRT breakup model is developed based on Eq. (14) to simulate ultra-high pressure diesel injection. This modified model has been added to the SprayFoam solver of the OpenFOAM freeware. The results produced by this new model have been compared against the default breakup model and validated by the available experimental data of Wang et al. [19].

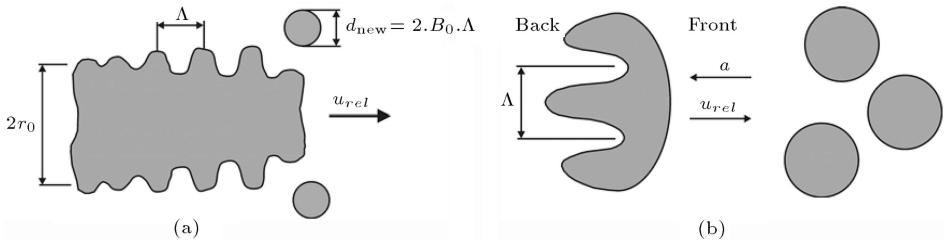

Figure 1. Schematics of Kelvin-Helmholtz model (a), and Rayleigh-Taylor instability (b) [1].

3. Computational model

A simple grading structured mesh has been used to simulate a single-hole injector under a set of conditions that was experimentally presented by Wang et al. [19]. The modified SprayFoam solver has been utilized to simulate high-pressure spray. The OpenFOAM 2.1.1 version has been used in this study and run in parallel using 16 processors. For validation of the current simulations, the nozzle diameter is taken to be 0.16 mm. The injector opens and closes rapidly and thus has top-hat injection rate profiles. Injection duration was set to be 1.5 ms. Ambient temperature was considered to be 295 K and fuel density was set equal to 830 kg/m^3. Three injection pressures of 100, 200, and 300 MPa were adopted.

The fuel properties of kerosene, which are based on experimental data of Wang et al., are presented in Table 1.

In general, theoretical studies have assumed that the injection rate shape is perfectly rectangular. However, in real cases, this is not completely true, since the mass flow rate curve is influenced by the dynamic behavior of the injector that depends on injection pressure and back pressure. Some authors have described the mass flow rate in the stabilized zone as:

$$\dot{m}_0 = C_{Di} A_0 \sqrt{2\rho(p_{inj} - p_b)}, \tag{19}$$

which has been previously introduced by Payri et al. [37]. Here, $\dot{m}_0$ is the mass flow rate, C_D is the discharge coefficient, A_0 is the nozzle orifice surface at the outlet, ρ is the fluid density, p_{inj} is the injection pressure, and p_b is the chamber pressure during the injection time. Figure 2 shows the fuel mass flow rate vs. time at the injection pressure of 300 MPa.

Table 1. Fuel properties [19].

Density (kg/m^3)	830
Kinematic viscosity (mm^2/s)	3.36
Surface tension (mN/m)	25.5
Nozzle diameter (μm)	160
Injection duration (ms)	1.5
Ambient gas temperature (K)	295

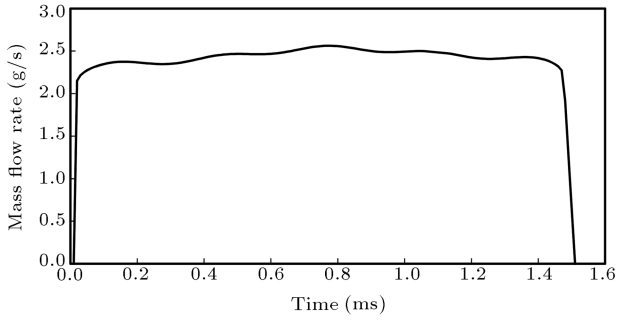

Figure 2. Injector mass flow rate for $P_{inj} = 300$ MPa.

3.1. Numerical uncertainty analysis

A constant volume chamber of size ($50 \times 50 \times 100$ mm^3) has been used, and, based on a grid independency study, 1.2×10^6 cells were applied to the considered domain. Also, numerical uncertainty has been estimated by applying the Celik [38] method. Three different grid sizes are selected and the obtained spray penetration is compared as the main key parameter of the current study. Based on the error estimation presented by Celik [38], the procedure of determining numerical uncertainty is described as follows:

1. Representative grid size, h, is defined as:

$$h = \left[\frac{1}{N}\sum_{i=1}^{N}(\Delta V_i)\right]^{1/3}, \tag{20}$$

where ΔV_i is volume of the ith cell, and N is the total number of cells.

2. Three different sets of grids are selected and the following equations are solved numerically to find the apparent order, p:

$$p = \frac{1}{\ln(r_{21})}|\ln|\varepsilon_{32}/\varepsilon_{21}| + q(p)|,$$

$$q(p) = \ln\left(\frac{r_{21}^p - s}{r_{32}^p - s}\right),$$

$$s = 1.\text{sign}(\varepsilon_{32}/\varepsilon_{21}), \tag{21}$$

where $r_{21} = h_2/h_1$, $r_{32} = h_3/h_2$ ($h_1 < h_2 < h_3$), $\varepsilon_{21} = \phi_2 - \phi_1$ and $\varepsilon_{32} = \phi_3 - \phi_2$.

3. Approximate relative error is defined as:

$$e_a^{21} = \left|\frac{\phi_1 - \phi_2}{\phi_1}\right|. \tag{22}$$

4. The convergence index is defined as:

$$GCI_{\text{fine}}^{21} = \frac{1.25 e_a^{21}}{r_{21}^p - 1}. \tag{23}$$

This index is considered as numerical uncertainty.

Spray penetration at various time steps, error, and the convergence index of these simulations ($P_{inj} = 300$ MPa) are presented in Table 1. According to Table 2, numerical uncertainty for spray penetration in a finer-grid solution is approximately 9.8, 3.1 and 2 percent for times 0.4, 0.6, and 0.8 ms after the start of injection.

4. Results and discussion

Spray tip penetration and spray angle are two of the most described spray characteristics in the literature. Penetration length is defined as the distance between

Table 2. Calculation of discretization error at three time steps.

	$t = 0.4$ ms (ASOI)	$t = 0.6$ ms (ASOI)	$t = 0.8$ ms (ASOI)
N_1	5×10^5	5×10^5	5×10^5
N_2	1.5×10^6	1.5×10^6	1.5×10^6
N_3	3.5×10^6	3.5×10^6	3.5×10^6
ϕ_1^*	52	65	75
ϕ_2	55	69	78
ϕ_3	56	70	78.5
GCI_{fine}^{21}	0.098	0.03079	0.02002

*ϕ is spray penetration (mm) for $p_{inj} = 300$ MPa.

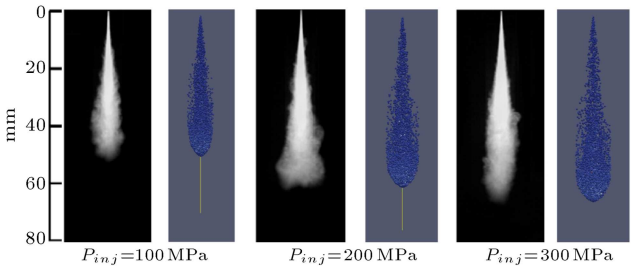

Figure 3. Comparison of the numerical results under various injection pressures (for each pressure: left (Exp.), right (Num.)) at $t = 0.7$ ms and $\rho_{amb} = 15$ kg/m^3 against the experimental jet penetration shapes [19].

the nozzle and the farthest axial location of the spray boundary. Also, spray angle is measured based on the radial distance at the axial location of 40 mm.

In order to examine the capability of the current model in predicting spray characteristics under ultra-high-pressure conditions, the produced results are compared against experimental measurements for non-evaporating and non-reacting sprays. Figure 3 presents a set of spray images and numerical results at $t = 0.7$ ms for various injection pressures. The spray shape is compared against experimental results of Wang et al. [19]. As observed in this figure, spray shape, droplet penetration and radial dispersion are in good agreement with the experimentally captured images of considered cases.

Spray tip penetration, as a function of time, is perhaps the most common quantity to study in the field of diesel spray research, since the tip position can be easily detected from spray shadowgraph images. Figure 4 shows the effect of the breakup model on the spray shape for the injection pressure and ambient density of 100 MPa and 15 kg/m^3 at $t = 1.0$ ms after the start of injection. It is quite evident that the modified KHRT model presents more acceptable spray shape and penetration.

Figure 5 illustrates a comparison of the current spray tip penetration against the experimental measurements of Wang et al. [19] for various injection

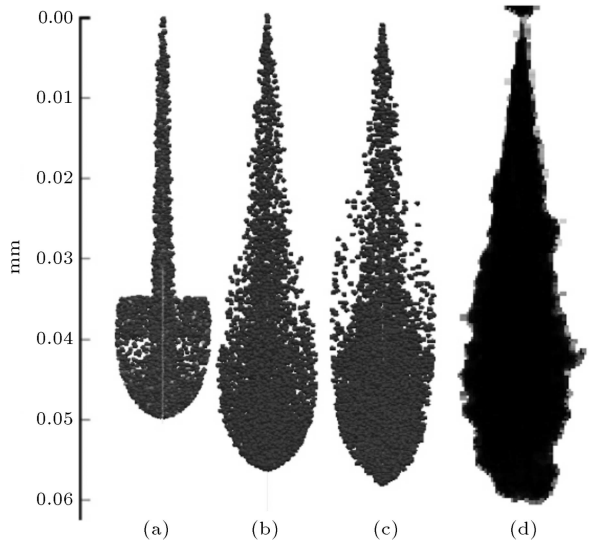

Figure 4. Comparison of spray shapes of different breakup models with experimental data [19]: (a) Pilch-Erdman; (b) default KHRT; (c) modified KHRT; and (d) experiments.

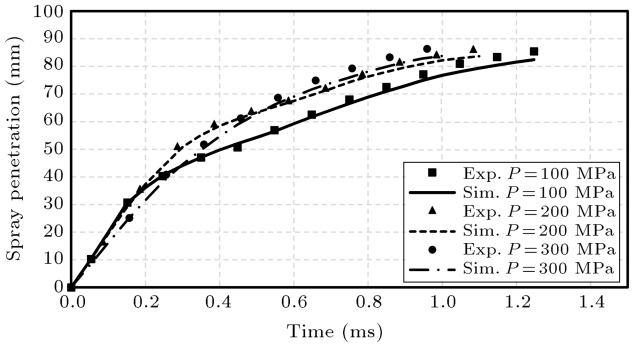

Figure 5. Comparison of spray jet penetration length of current simulation with Wang et al. findings [19].

pressures under ambient density of 15 kg/m^3. It can be observed in this figure that the numerical jet fuel penetration distance agrees well with the experimental data. Root Mean Square Errors (RMSE) are 1.72, 1.73 and 2.21 for injection pressures of 100, 200 and 300 MPa, respectively. It is quite evident that increasing injection pressure leads to higher values of jet penetration. Also, prediction of penetration at initial times after the start of injection seems to be more accurate. The spray tip penetration clearly increases when the injection pressure increases from 100 to 200 MPa. This increase seems to be very moderate, from 200 to 300 MPa.

The effects of ambient density on spray tip penetration have been presented in Figure 6. Higher spray penetrations have been achieved under high spray density. On the other hand, increasing the nozzle hole diameter leads to higher fuel mass flow rate and, thus, higher spray penetration, as shown in Figure 7.

Average spray angles for each injection pressure

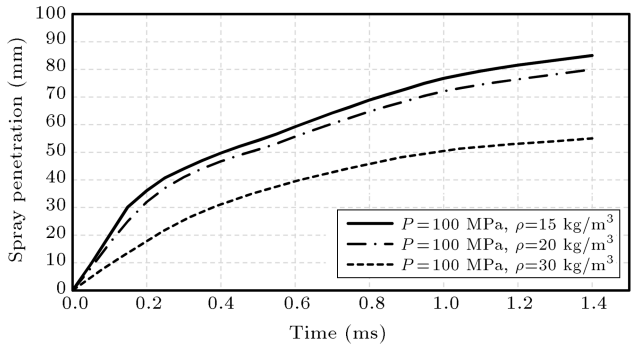

Figure 6. Effects of ambient density on spray tip penetration.

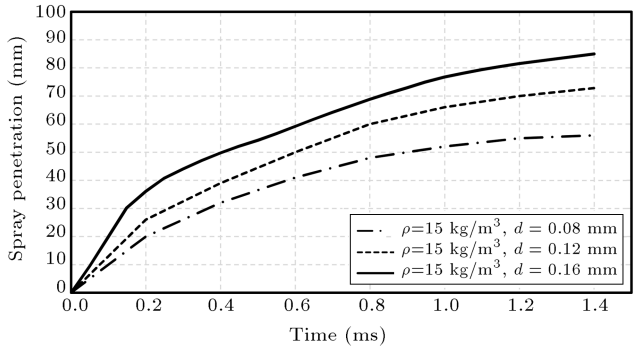

Figure 7. Effects of nozzle hole diameter on spray tip penetration.

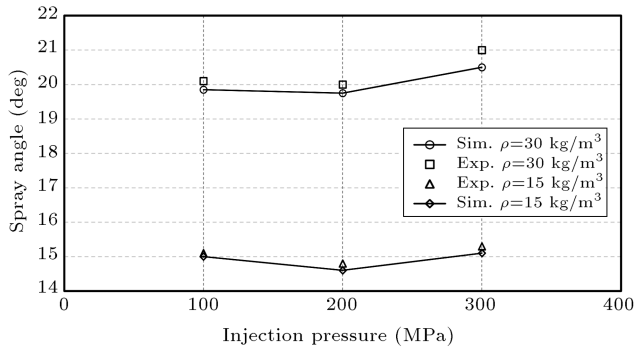

Figure 8. Comparison of the average spray angle under various injection pressures ($d = 0.16$ mm).

for two different ambient densities and 0.16 mm nozzle diameter are presented in Figure 8. From this figure, one may conclude that the spray angle is not sensitive to injection pressure. Injection pressure appears to have little influence on diesel spray angle and remains nearly constant during the whole injection. On the other hand, ambient condition is an effective parameter on spray angle. The effects of nozzle diameter on spray angle are shown in Figure 9. As evident in this figure, increasing the nozzle hole diameter leads to higher values of spray angle.

To further understand the spray morphology, spray volume is estimated and presented in Figure 10. Spray volume can be described by the relation [39].

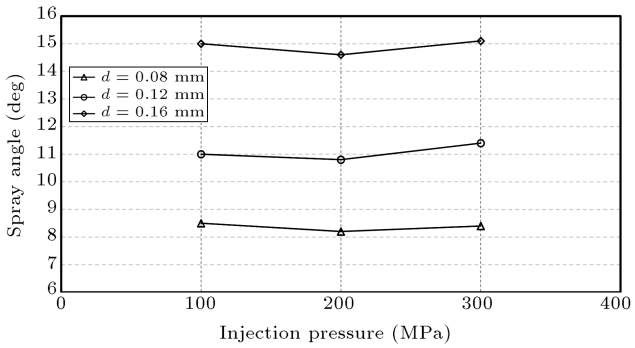

Figure 9. Effects of nozzle hole diameter on average spray angle under various injection pressures ($\rho_{amb} = 15$ kg/m^3).

$$V(t) = \frac{1}{3}\pi S^3(t)\tan^2\left(\frac{\theta}{2}\right)\frac{\left(1+2\tan\left(\frac{\theta}{2}\right)\right)}{\left(1+\tan\left(\frac{\theta}{2}\right)\right)^3}. \tag{24}$$

Comparison of the numerical results of spray volume under different pressures (100, 200, and 300 MPa) with the experimental data in Figure 10 indicates good agreement. Similar to the case of spray penetration, RMSE values are below 3 for the spray volume. Based on the experimental data presented by Wang et al. [19], to eliminate the influence of injection timing on spray area, the spray area is plotted versus the spray tip penetration.

The obtained results show that spray volume has been affected by spray angle and penetration. Therefore, injection pressure has little effect on spray volume and it is expected that increasing the ambient density and nozzle diameter leads to higher spray volumes. Figure 11 illustrate the effects of ambient density on spray volume.

The total amount of air entrained up to any axial location in a fuel jet relative to the amount of injected fuel is estimated using formula [39]:

$$\bar{\phi}(x) = \frac{2(A/F)_{st}}{\sqrt{1+16(x/x^+)^2}-1}, \tag{25}$$

where $\bar{\phi}$ is the averaged cross-sectional equivalence ratio at any axial location of x. $(A/F)_{st}$ is the stoichiometric air/fuel ratio (14.69 for diesel fuel [19]), and x^+ is the characteristic length scale for the fuel jet, as in:

$$x^+ = \sqrt{\frac{\rho_f}{\rho_a}}\frac{\sqrt{C_a}d_0}{a\tan(\theta/2)}, \tag{26}$$

where C_a is the orifice area contraction coefficient, which is assumed to be 0.95 in this study [37], and a is constant, with a value of 0.75.

Figure 12 illustrates the averaged cross-sectional equivalence ratio at any axial location. It is evident that increasing the ambient density leads to lower equivalent ratio.

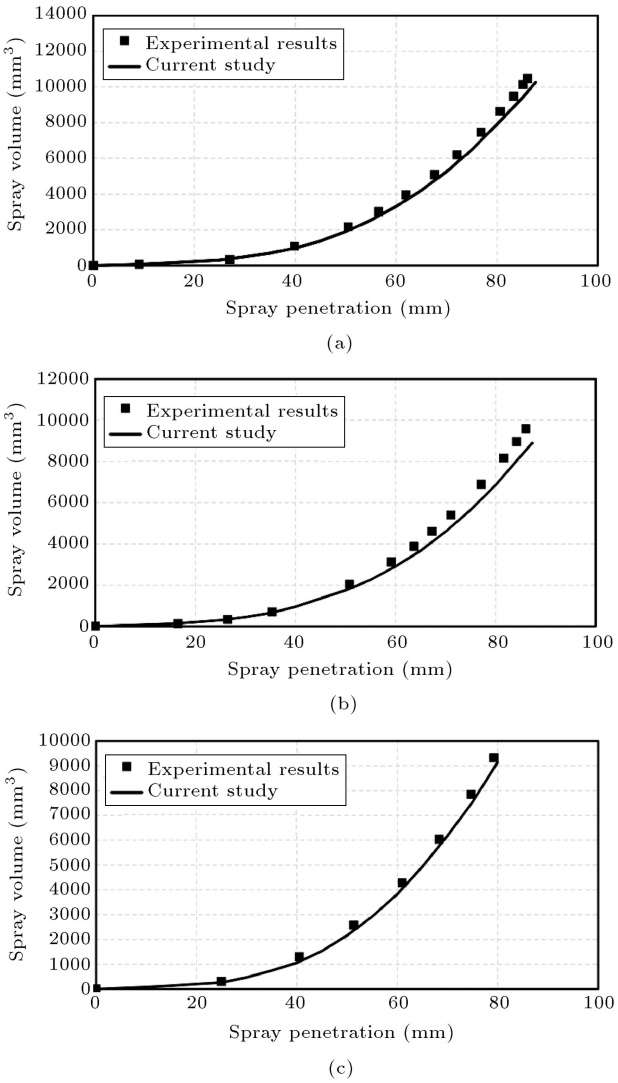

Figure 10. Comparison of the numerical and experimental results of spray volume in terms of spray jet penetration length at (a) 100 MPa, (b) 200 MPa, and (c) 300 MPa.

Further insight into the breakup process can be gained by examining the droplet size predictions. Sauter Mean Diameter (SMD) is defined as the diameter of a sphere that has the same volume/surface area ratio as the entire spray. The SMD correlation has been presented by Ejim et al. [40] as in:

$$\text{SMD} = 6156 v^{0.385} \sigma^{0.737} \rho_f^{0.737} \rho_a^{0.06} \Delta P^{-0.54}, \qquad (27)$$

where v and σ are viscosity and surface tension, and ΔP is the difference between injection and ambient pressures. The effect of injection pressure on SMD for various injection pressures is presented in Figure 13.

At the start of injection, SMD is close to the nozzle size and then sharply reduces, as a result of the breakup process. As shown in Figure 10, higher spray injection leads to smaller droplet size. SMD values match the analytic data under high injection pressure.

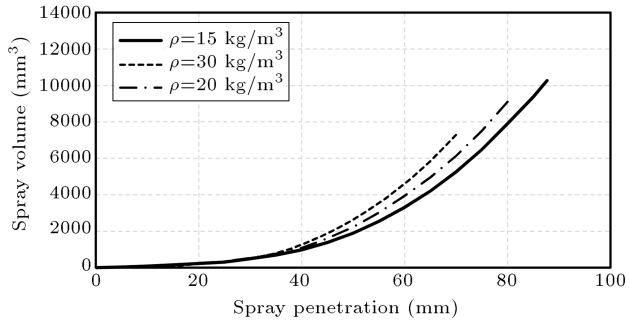

Figure 11. Effects of ambient density on spray volume for $P_{inj} = 100$ MPa and $d = 0.16$ mm.

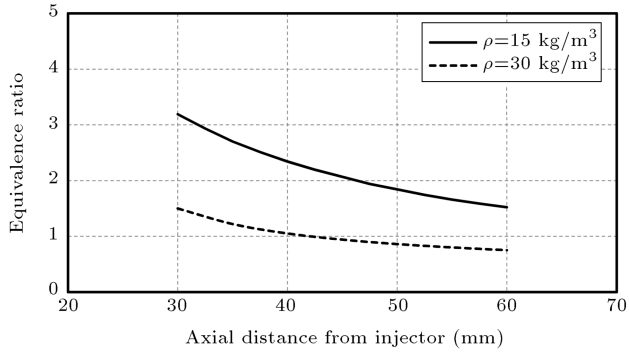

Figure 12. Equivalence ratio along the injector axis ($P_{inj} = 100$ MPa, $d = 0.16$ mm).

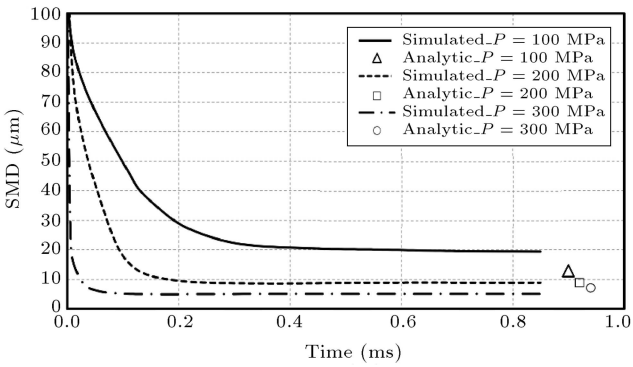

Figure 13. Effect of injection pressure on SMD ($P_{inj} = 100$ MPa, $d = 0.16$ mm).

Based on the numerical results of spray penetration, spray angle and spray volume, and their favorable agreement with existing experimental data, for which maximum RMSE is below 3, one may suggest that the proposed solver and the applied sub-models are suitable tools for accurate simulation of ultra-high pressure diesel spray.

5. Conclusions

A numerical investigation has been performed, based on three dimensional CFD simulations, for validation of the atomization model of a single hole nozzle and symmetric diesel spray under ultra-high pressures

and non-evaporating and non-reacting conditions. A Lagrangian particle tracking scheme has been implemented for the liquid droplet modeling, and the RANS method has been used to simulate the gas field. The SpraydFoam solver of the OpenFOAM open source code has been modified to consider the transient effects of ultra-high injection pressures, based on a valid scheme. A comprehensive study of the effects of different parameters, such as fuel injection pressure, ambient gas density, and nozzle hole diameter, on spray characteristics has been conducted. The new modified breakup model presented more accurate results in the case of ultra-high injection pressures. Based on the acquired results, it is concluded that fuel pressure, ambient density and nozzle diameter have the greatest effect on spray penetration length. The spray tip penetration clearly increases when the injection pressure increases from 100 to 200 MPa. This increase seems to be very moderate, from 200 to 300 MPa. Higher spray penetrations have been achieved under high spray density. Increasing the nozzle hole diameter leads to higher fuel mass flow rate and higher spray penetration. Injection pressure appears to have little influence on diesel spray angle and remains nearly constant during the whole injection. On the other hand, ambient condition is seen to be an effective parameter on the spray angle.

The aim of the present study has been to generate a model for accurately predicting spray shapes and properties, especially at ultra-high injection pressures. High injection pressure breaks droplets into smaller sizes, thus slightly reducing spray penetration. As a result, a higher dispersion rate is predicted. Meanwhile, increasing injection pressure leads to small droplets and a decrease in Sauter Mean Diameter (SMD). Good agreement has been achieved between the proposed numerical model and the experimental measurements reported in the literature. The maximum value of the Root Mean Square Error (RMSE) is determined to be below 3 for the spray penetration and volume. In conclusion, it is also found that the proposed Eulerian-Lagrangian scheme, using RANS formulation for the continuous field, and the new advanced composite breakup model are appropriate for simulation of a very high direct injection pressure.

Nomenclature

A_o	Nozzle orifice surface (m^2)
B_0	Breakup constant
B_1	Breakup constant
C_D	Drag constant
C_{Di}	Discharge coefficient
E	Total energy per unit volume
g	Body force per unit of mass
L_b	Breakup length (m)
Oh	Ohnesorge number
$\dot{m}_o$	Mass flow rate ($kg.s^{-1}$)
p	Pressure (Pa)
p_b	Chamber pressure (Pa)
p_{inj}	Injection pressure (Pa)
Pr	Prandtl number
q	Heat flux vector
r_0	Droplet radius before breakup (m)
r_c	Radius of child droplets (m)
Re_p	Particle Reynolds number
Re_l	Liquid Reynolds number
S_{ij}	Rate-of-strain tensor
Ta	Taylor number
u	Fluid velocity ($m.s^{-1}$)
u_p	Particle velocity ($m.s^{-1}$)
u_g	Gas velocity ($m.s^{-1}$)
U_m	Jet velocity ($m.s^{-1}$)
We_g	Gas Weber number
We_l	Liquid Weber number

Greek letters

Λ_{KH}	Kelvin-Helmholtz wavelength (m)
Ω_{KH}	Kelvin-Helmholtz growth rate (s^{-1})
Λ_{RT}	Rayleigh-Taylor wavelength (m)
Ω_{RT}	Rayleigh-Taylor growth rate (s^{-1})
μ	Dynamic viscosity ($kg.m^{-1}.s^{-1}$)
v	Kinematic viscosity ($m^2.s^{-1}$)
ρ	Density ($kg.m^{-3}$)
ρ_p	Particle density ($kg.m^{-3}$)
τ_{bu}	Breakup time (s)
τ_{ij}	Stress tensor ($kg.m^{-1}.s^{-2}$)
τ_{KH}	Kelvin-Helmholtz breakup time (s)

References

1. Baumgarten, C., *Mixture Formation in Internal Combustion Engine*, Springer, New York (2006).
2. Reitz, R.D. and Bracco, F.V. "Mechanism of atomization of a liquid", *Jet. Physics of Fluids*, **25**, pp. 1730-1741 (1982).
3. Wan, Y. and Peters, N. "Scaling of spray penetration with evaporation", *Atomization and Sprays*, **9**(2), pp. 111-132 (1999).
4. Som, S. and Aggarwal, S.K. "Effects of primary breakup modeling on spray and combustion characteristics of compression ignition engines", *Combustion and Flame*, **157**, pp. 1179-1193 (2010).

5. Hosseinpour, S. and Binesh, A.R. "Investigation of fuel spray atomization in a DI heavy-duty diesel engine and comparison of various spray breakup model", *Fuel*, **88**, pp. 799-805 (2009).

6. Som, S., Aggarwal, S.K., El-Hannouny, E.M. and Longman, D.E. "Investigation of nozzle flow and cavitation characteristics in a diesel injector", *ASME J. Eng. Gas Turbines Power*, **132**, 042802 (2010).

7. Ishii, E., Ishikawa, M., Sukegawa, Y. and Yamada, H. "Secondary-drop-breakup simulation integrated with fuel-breakup simulation near injector outlet", *ASME J. Fluids Eng.*, **133**(8), 081302 (2011).

8. Desantes, J.M., Payri, R., Garcia, J.M. and Salvador, F.J. "A contribution to the understanding of isothermal diesel spray dynamics", *Fuel*, **86**(7-8), pp. 1093-1101 (2007).

9. Turner, M.R., Sazhin, S.S., Healey, J.J., Crua, C. and Martynov, S.B "A breakup model for transient diesel fuel sprays", *Fuel*, **97**, pp. 288-305 (2012).

10. Yadollahi, B. and Boroomand, M. "Multidimensional modeling of CNG direct injection and mixture preparation in a SI engine cylinder", *Scientia Iranica B*, **20**(6), pp. 1729-1741 (2013).

11. Mohammadebrahima, A., Kazemzadeh Hannania, S. and Shafii, B. "Investigation into the effect of intake port geometric parameters and blockage on flow coefficient and in-cylinder flow: Application to engine port design", *Scientia Iranica B*, **21**(2), pp. 438-448 (2014).

12. Ghasemi, A., Barron, R.M. and Balachandar, R. "Spray-induced air motion in single and twin ultra-high injection diesel sprays", *Fuel*, **121**, pp. 284-297 (2014).

13. Kato, T., Tsujimura, K., Shintani, K., Minami, T. and Yamaguchi, I. "Spray characteristics and combustion improvement of D.I. diesel engine with high pressure fuel injection", SAE Technical Paper 890265 (1989).

14. Yokota, T., Kamimoto, T., Kosaka, H. and Tsujimura, K. "Fast burning and reduced soot formation via ultra-high pressure diesel fuel injection", SAE Paper No. 910225 (1991).

15. Benajes, J., Pastor, J.V., Payri, R. and Plazas, A.H. "Analysis of the influence of diesel nozzle geometry in the injection rate characteristic," *ASME J. Fluids Eng.*, **126**, pp. 63-71 (2004).

16. Kastengren, A.L., Powell, C.F., Riedel, T., Cheong, S.-K., I.M, K.-S., Liu, X., Wang, Y.J. and Wang, J. "Nozzle geometry and injection duration effects on diesel sprays measured by X-ray radiography", *ASME J. Fluids Eng.*, **130**(4), 041301 (2008).

17. Lee, S.H., Jeong, D.Y, Lee, J.T., Ryou, H.S. and Hong, K. "Investigation on spray characteristics under ultra-high injection pressure conditions", *International Journal of Automotive Technology*, **6**(2), pp. 125-131 (2005).

18. Tao, F. and Bergstrand, P. "Effect of injection pressure on diesel ignition and flame under high-boost conditions", SAE Paper No. 2008-01-1603 (2008).

19. Wang, X., Huang, Z., Kuti, O.A., Zhang, W. and Nishida, K. "Experimental and analytical study on biodiesel and diesel spray characteristics under ultra-high injection pressure", *Int. J. Heat Fluid Flow*, **31**, pp. 659-666 (2010).

20. Roisman, I.V., Araneo, L. and Tropea, C. "Effect of ambient pressure on penetration of a diesel spray", *International Journal of Multiphase Flow*, **33**, pp. 904-920 (2007).

21. Zhu, J., Kuti, O.A. and Nishida, K. "An investigation of the effects of fuel injection pressure, ambient gas density and nozzle hole diameter on surrounding gas flow of a single diesel spray by the laser-induced fluorescence-particle image velocimetry technique", *International Journal of Engine Research*, **14**(6), pp. 630-645 (2012).

22. Shervani-Tabar, M.T., Sheykhvazayefi, M. and Ghorbani, M. "Numerical study on the effect of the injection pressure on spray penetration length", *Applied Mathematical Modelling*, **37**, pp. 7778-7788 (2013).

23. Gjesing, R., Hattel, J. and Fritsching, U. "Coupled atomization and spray modelling in the spray forming process using OpenFOAM", *Engineering Applications of Computational Fluid Mechanics*, **3**(4), pp. 471-486 (2009).

24. Kassem, H.I., Saqr, K.M., Aly, H.S., Sies, M.M. and Wahid, M.A. "Implementation of the eddy dissipation model of turbulent non-premixed combustion in OpenFOAM", *International Communications in Heat and Mass Transfer*, **38**, pp. 363-367 (2011).

25. Vuorinen, V., Duwig, C., Fuchs, L. and Larmi, M. "Large-eddy simulation of a compressible spray using Eulerian-Eulerian approach", *24th European Conference on Liquid Atomization and Spray Systems*, Estoril, Portugal (2011).

26. Nowruzi, H., Ghadimi, P. and Yousefifard, M. "A numerical study of spray characteristics in medium speed engine fueled by different HFO/n-butanol blends", *International Journal of Chemical Engineering*, Article ID: 702890 (2014).

27. Yousefifard, M., Ghadimi, P. and Mirsalim, M. "Numerical simulation of biodiesel spray under ultra-high injection pressure using OpenFOAM", *Journal of the Brazilian Society of Mechanical Sciences and Engineering*, **37**, pp. 737-746 (2015).

28. Yousefifard, M., Ghadimi, P. and Nowruzi, H. "Three-dimensional LES modeling of induced gas motion under the influence of injection pressure and ambient density in an ultrahigh-pressure diesel injector", *Journal of the Brazilian Society of Mechanical Sciences and Engineering*, DOI 10.1007/s40430-014-0246-8 (2014).

29. Versteeg, H.K. and Malalasekera, W. "An introduction to computational fluid dynamics: The finite volume

method", *Longman Scientific & Technical*, New York (2007).

30. Stiesch, G., *Modeling Engine Spray and Combustion Processes*, Springer (2003).
31. Pope, S.B., *Turbulent Flows*, Cambridge University Press, Cambridge (2001).
32. Ferziger, J.H. and Peric, M., *Computational Methods for Fluid Dynamics*, Springer, New York (2002).
33. Jones, W.P. and Launder, B.E. "The prediction of laminarization with a two-equation model of turbulence", *International Journal of Heat and Mass Transfer*, **15**, pp. 301-314 (1972).
34. Reitz, R.D. "Modeling atomization processes in high-pressure vaporizing sprays", *Atomization and Spray Technology*, **3**, pp. 309-337 (1987).
35. Sazhin, S.S., Martynov, S.B., Kristyadi, T., Crua, C. and Heikal, M.R. "Diesel fuel spray penetration, heating, evaporation and ignition: Modeling versus experimentation", *Int. J. Engineering Systems and Modelling*, **1**(1), pp. 1-19 (2008).
36. Bellman, R. and Pennington, R. "Effects of surface tension and viscosity on Taylor instability", *Quart. Appl. Math.*, **12**, pp. 151-162 (1954).
37. Payri, R., Garcia, J.M., Salvador, J. and Gimeno, J. "Using spray momentum flux measurements to understand the influence of diesel nozzle geometry on spray characteristics", *Fuel*, **84**, pp. 551-561 (2005).
38. Celik, I. "Numerical uncertainty in fluid flow calculations: Needs for future research", *ASME Journal of Fluid Engineering*, **115**, pp. 194-195 (1993).
39. Naber, J.D. and Siebers, D.L. "Effects of gas density and vaporization on penetration and dispersion of diesel sprays", SAE Technical Paper 960034 (1996).
40. Ejim, C.M., Fleck, B.A. and Amirfazli, A. "Analytical study for atomization of biodiesels and their blends in a typical injector: Surface tension and viscosity effects", *Fuel*, **86**, pp. 1534-1544 (2007).

Biographies

Mahdi Yousefifard received his BS degree in Naval Engineering from the Persian Gulf University, Bushehr, Iran, in 2003, and an MS degree in Naval Architecural Engineering from Sharif University of Technology, Tehran, Iran, in 2005. He is currently a PhD degree candidate in the Marine Technology Faculty of Amirkabir University of Technology (AUT), Tehran, Iran. His research interests include CFD modeling of high pressure diesel injection. He has published five scientific papers in the field of computational fluid dynamics of one and two-phase flows.

Parviz Ghadimi received his PhD degree in Mechanical Engineering, in 1994, from Duke University, USA. He served one year as Research Assistant Professor in M.E. and six years as a Visiting Assistant Professor in the Mathematics Department at Duke. He is currently Associate Professor of Hydromechanics in the Department of Marine Technology at Amirkabir University of Technology, Tehran, Iran. His main research interests include hydrodynamics, hydroacoustics, thermo-hydrodynamics, and CFD, and he has authored several scientific papers in these fields. He has also authored two textbooks in Farsi; Applied Computational Fluid Dynamics and Engineering Mathematics.

Seyyed Mostafa Mirsalim received his BS and MS degrees in Mechanical Engineering from the University of Poitiers France, in 1967 and 1969, respectively. He received his certificate in Thermodynamics and Fluid Mechanic, in 1970, from the same university. He is currently Assistant Professor in the Department. of Mechanical Engineering at Amirkabir University of Technology, Tehran, Iran. He has published two Farsi language reference books on Internal Combustion Engines and Gas Engines and published and presented over fifty scientific articles in international journals and at different national and international conferences.